An Experimental Assessment of Robust control and Estimation of Acetate Concentration in Escherichia coli BL21(DE3) Fed-batch Cultures

Merouane Abadli, Laurent Dewasme, Sihem Tebbani, Didier Dumur, Alain Vande Wouwer

Version of Record: https://www.sciencedirect.com/science/article/pii/S1369703X21001790
Manuscript_996f0814c1faa02347c57abf413eae9a

An Experimental Assessment of Robust control and Estimation of Acetate Concentration in *Escherichia coli* BL21(DE3) Fed-batch Cultures

Merouane Abadli[a,b], Laurent Dewasme[b], Sihem Tebbani[a], Didier Dumur[a], Alain Vande Wouwer[b]

[a] *Université Paris-Saclay, CNRS, CentraleSupélec, Laboratoire des Signaux et Systèmes, 3 rue Joliot-Curie, 91192 Gif sur Yvette, France*
[b] *Systems, Estimation, Control and Optimization (SECO), University of Mons, 31, Boulevard Dolez , 7000 Mons, Belgium;*

Abstract

Avoiding acetate accumulation is a major challenge in *Escherichia coli* fed-batch cultures, since it leads to an inhibition of the cell respiratory capacity. A closed-loop regulation ensuring a low acetate concentration offers a practical solution to maintain the cultures near the optimal operating conditions.

In this work, a robust Generic Model Controller (GMC) is designed and implemented to regulate the acetate concentration in *E. coli* BL21 (DE3) fed-batch cultures. To compensate for model mismatch, disturbances, and measurement noise, a robust design using the $\mathcal{LMI}$ formalism is achieved, considering robustness and transient performance requirements. Since the acetate concentration is not available for on-line measurement, an Unscented Kalman Filter (UKF) is also designed and implemented to estimate the acetate concentration based on an on-line biomass measurement.

The proposed GMC-UKF strategy is validated through simulation runs and experimental tests at lab-scale. The control strategy shows good performance in regulating the non-measured acetate concentration. The estimation of this latter signal from the biomass measurement is performed accurately by the UKF.

Keywords: Feedback Linearization, Process Control, Kalman Filter, Biotechnology

1. Introduction

Recombinant proteins are widely used to produce a vast array of biopharmaceutical products. One of the common ways to achieve industrial-scale production is through fed-batch cultivation of genetically modified strains of *Escherichia coli*. The operational advantage is the scalable process, the low operational costs, and the relatively simple media conditions. On the other hand, *Escherichia coli* is known for its physiological and biological features, such as flexible culture conditions, fast growth and high production yields [1, 2].

The main challenge to ensure the process efficiency and productivity is the accumulation of acetate, a metabolic by-product inhibiting cell growth [3]. Acetate formation occurs when the capacity for energy generation within the cell is exceeded, due to high flux into the main metabolic pathways caused by an excess in the carbon source [4, 5]. This mechanism is referred to as overflow metabolism [6].

Acetate presence in high concentration causes the inhibition of the cell respiratory capacity, leading to the decrease of biomass production yield and consequently the decrease of the recombinant protein production [7, 8].

Keeping the feeding at a sufficiently low rate prevents acetate formation, but can lead to low productivity and a long cultivation time. It is therefore required to determine a feeding profile that maximizes biomass productivity while avoiding overflow metabolism [9].

Several optimization strategies and process control architectures have been developed to reduce or avoid overflow metabolism [10–17]. Basically, two different approaches can be followed. The first approach consists in controlling the specific biomass growth rate [18, 19] and to impose a reference biomass evolution profile. This type of control is made possible by the availability of reliable on-line biomass probes which allow convenient real-time implementation. However, the definition of a biomass reference profile is not straightforward as it relies on prior process knowledge (i.e., a growth model based on past experimental observations), and in practice, a suboptimal solution is often selected such as to ensure sufficient margin of security. Limiting the specific growth rate presents some practical and metabolic limitations, since its maximal level depends on the oxidative capacity of the cells which is by essence, uncertain. Therefore, targeting a growth rate close to its maximal value could lead to several uncontrolled metabolic switches provoking latencies. An example can be found in [20] where the glucose and oxygen consumption rates and CO_2 evolution rate suddenly and reproducibly decreased, causing a break of the metabolism for a period of 40 min, and a drop in the biomass productivity.

The second approach consists in regulating, either the substrate or the by-product concentration at specific levels [14–16]. The substrate concentration should be close to a threshold corresponding to the critical oxidation capacity, while the by-production concentration should be close to zero. The main obstacle is the difficulty of on-line implementation, due to the requirement of accurate measurements of low-level concentrations

of acetate and/or glucose.

It is reported in [21] that industrially relevant inhibitory levels of acetate concentration are on the order of 100 mM (6 g/L). The authors studied the effect of acetate presence in the culture medium on *E. coli* metabolism and showed that a concentration of 16.67 mM (1 g/L) corresponds to less than 20% drop in the growth rate compared to its maximal value.

In this context, the contribution of this paper is twofold:

- to propose a control strategy combining robust linearizing control with a software sensor to monitor and regulate the acetate concentration on-line. In this way, the need of an accurate process model is less pressing, and acetate concentration can be reconstructed from the biomass signal.

- to develop a proof of concept through experimental runs at lab-scale. Indeed, even though several control paradigms have been proposed in earlier publications there is a dire lack of reports on experimental validation, most of the published results being based on simulation studies.

To the authors' knowledge, the only successful report of an experimental application of linearizing control to fed-batch cultures of *Escherichia coli* cultures is published in [10], where the acetate concentration is regulated to a pre-defined set-point. However, the control strategy relies on an accurate knowledge of the model parameters, which is a major drawback since a bioprocess model is always uncertain. Parameter adaptation strategies are usually applied to compensate the uncertainty in the kinetic terms of the process model. However, stability is not guaranteed in presence of unmodeled dynamics and high noise levels, and this is why we propose a robust $\mathcal{LMI}$-based linearizing control, which will be able to alleviate this difficulty. Moreover, the control loop developed in [10] is based on a flux injection analysis (FIA) device, whose market distribution has long been disrupted, and no other similar device has been (re)developed in the meantime. The use of state estimation, or software sensors, seems therefore the most appropriate solution to avoid the burden of complex, unreliable, sensing techniques. The results reported in [10] show that exponential growth could not be sustained in the experimental studies, which might be an indication of the lack of accuracy of the FIA device. In this study, we propose an Unscented Kalman Filter (UKF) for the online recontruction of the acetate concentration.

More specifically, we aim at the development of Generic Model Control (GMC) [22], which is an adaptive control strategy based on feedback linearization, embedding the process non-linearities in the design of the control law. GMC has been used in several process control applications, e.g. [23] where it was applied to track the foreign protein level reference trajectory in *E. coli* fermentations, [24] where is was applied to anaerobic digestion, and [25] where dual product composition was controlled in an industrial high purity distillation column. In this study, a robust version of the Generic Model Control

(GMC) strategy is developed to control the acetate concentration to a low predefined value. $\mathcal{LMI}$s are considered in the control synthesis to derive the GMC control gains. The control design includes performance requirements using the regional pole placement technique. The approach ensures both the robust stability of the process in presence of model uncertainties and measurement noise, and the desired transient performance of the closed-loop system.

This paper is organized as follows. In section 2, the mechanistic model describing *E. coli* growth is presented. The Generic Model Control strategy is presented and applied to the *E. coli* model in section 3. In section 4, the robust control design approach with the $\mathcal{LMI}$s formulation is presented. Process observability analysis and acetate estimation using an Unscented Kalman Filter (UKF) are developed in section 5. Numerical simulation results are illustrated in section 6. Section 7 presents the materials and methods and experimental results are detailed and discussed in section 8. Conclusions and perspectives end this study in section 9.

2. Process dynamic model

In this section, we consider a generic mechanistic model describing *E. coli* growth in fed-batch cultures.

This model describes *E. coli* cells catabolism through the following three main reactions [26]:

$$k_{S1}S + k_{O1}O \xrightarrow{\mu_1\ X} k_{X1}X + k_{C1}C \tag{1a}$$

$$k_{S2}S + k_{O2}O \xrightarrow{\mu_2\ X} k_{X2}X + k_{A2}A + k_{C2}C \tag{1b}$$

$$k_{A3}A + k_{O3}O \xrightarrow{\mu_3\ X} k_{X3}X + k_{C3}C \tag{1c}$$

where X, S, A, O, C are respectively, the concentrations in the culture medium of biomass, substrate (glucose), acetate, dissolved oxygen, and carbon dioxide. $k_{\xi i}(\xi = X, S, A, O, C\ ;\ i = 1, 2, 3)$ are the yield coefficients. μ_1, μ_2, and μ_3 are the specific rates related to the catabolic reactions describing substrate oxidation (1a), acetate production (fermentation) (1b), and acetate oxidation (1c) [27]. Their proposed kinetic structures read: [28]:

$$\mu_1 = \frac{min(q_s, q_{s_{crit}})}{k_{S1}} \tag{2a}$$

$$\mu_2 = \frac{max(0, q_s - q_{s_{crit}})}{k_{S2}} \tag{2b}$$

$$\mu_3 = \frac{min(0, q_{AC})}{k_{A3}} \tag{2c}$$

The kinetic terms related to consumption rates $q_\star$ are defined by:

$$q_s = q_{s_{max}} \frac{S}{K_s + S} \tag{3a}$$

$$q_{s_{crit}} = \frac{q_{O_{max}}}{k_{OS}} \frac{K_{iA}}{K_{iA} + A} \tag{3b}$$

$$q_{AC} = \frac{k_{OS}(q_{s_{crit}} - q_s)}{k_{OA}} \frac{A}{K_A + A} \tag{3c}$$

where q_s and q_{AC} denote the substrate and acetate consumption rates respectively, $q_{s_{max}}$ and $q_{O_{max}}$ are the maximal consumption rates for substrate and dissolved oxygen respectively, and $q_{s_{crit}}$ represents the substrate critical consumption rate. In the following, mass balances are normalized with respect to the substrate and acetate ($k_{S1} = k_{S2} = k_{A3} = 1$).

The kinetic model (2) is based on the Sonnleitner and Käppeli bottleneck assumption [29], applied to *Saccharomyces cerevisiae* (Figure 1). Two different operating modes can be distinguished depending on the substrate concentration level. If the latter is higher than the critical threshold corresponding to the available oxidative capacity ($S > S_{crit}$), acetate is produced by the cells through the fermentative metabolic pathway (reactions (1a) and (1b)). The culture is said in respiro-fermentative mode (RF). Conversely, a substrate concentration lower than the critical threshold ($S < S_{crit}$) leads to substrate and acetate (if present in the culture medium) oxidation (reactions (1a) and (1c)), and the culture is said in respirative mode (R). When the substrate concentration is at the critical level and fills exactly the respirative capacity, the culture is in optimal conditions corresponding to the edge between the two operating modes, and acetate is neither produced nor consumed.

Applying component-wise mass balances to (1), we obtain the following differential equations [28]:

$$\dot{X} = (k_{X1}\mu_1 + k_{X2}\mu_2 + k_{X3}\mu_3)X - D\ X \tag{4a}$$

$$\dot{S} = -(\mu_1 + \mu_2)X - D\ (S - S_{in}) \tag{4b}$$

$$\dot{A} = (k_{A2}\mu_2 - \mu_3)X - D\ A \tag{4c}$$

$$\dot{O} = -(k_{O1}\mu_1 + k_{O2}\mu_2 + k_{O3}\mu_3)X - D\ O + OTR \tag{4d}$$

$$\dot{C} = (k_{C1}\mu_1 + k_{C2}\mu_2 + k_{C3}\mu_3)X - D\ C - CTR \tag{4e}$$

$$\dot{V} = F_{in} \tag{4f}$$

where S_{in} is the substrate concentration in the feed, and F_{in} is the inlet feed rate. V is the culture medium volume and D is the dilution rate ($D = \frac{F_{in}}{V}$).

OTR and CTR represent respectively the oxygen transfer rate from the gas phase to the liquid phase and the carbon transfer rate from the liquid phase to the gas phase, that can be modeled as follows [30]:

$$OTR = k_L a_O \left(O_{sat} - O\right) \tag{5}$$
$$CTR = k_L a_{CO_2} \left(C - C_{sat}\right) \tag{6}$$

where $k_L a_O$ and $k_L a_{CO_2}$ are respectively the volumetric transfer coefficients of oxygen and carbon dioxide. O_{sat} and C_{sat} are respectively the dissolved oxygen and carbon dioxide concentrations at saturation.

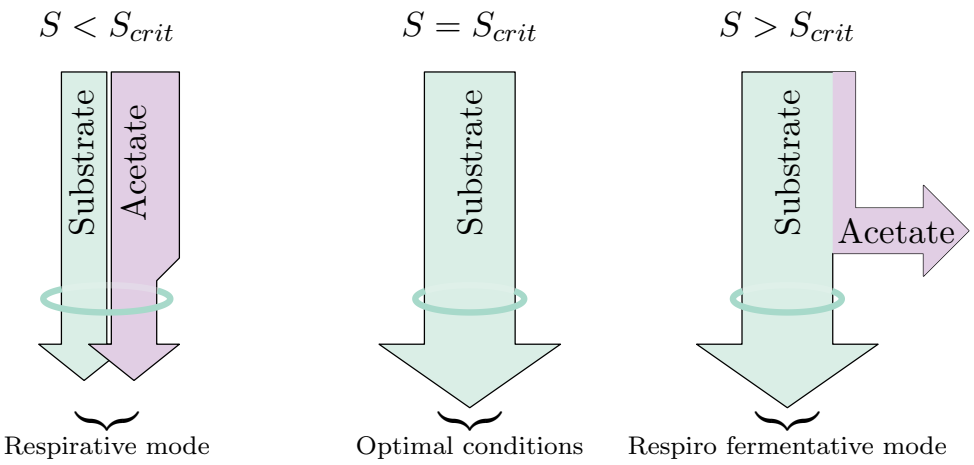

Figure 1: Illustration of the bottleneck assumption ([29]) describing the limited respiratory capacity

The optimal operating conditions maximizing the biomass productivity are at the boundary of the respiro-fermentative and respirative modes [14], where all the available substrate is assumed to be allocated for biomass production. Thus, the specific fermentation rate μ_2 and the specific acetate oxidation rate μ_3 are equal to zero:

$$\mu_1 = q_s = q_{s_{crit}} \tag{7}$$
$$\mu_2 = 0 \tag{8}$$
$$\mu_3 = 0 \tag{9}$$

Maintaining the culture at the edge between the respirative and respiro-fermentative modes requires controlling the substrate concentration to the critical value S_{crit}. An efficient on-line substrate measurement around this value is required [14], but the concentration level is below the resolution of currently available glucose probes.

At the optimal operating conditions, the acetate quantity (VA) is constant. However, the volume evolution is exponential, and the acetate concentration must therefore decrease with the same rate to maintain VA constant and reach the optimal operating conditions. This is a difficult task, especially at a concentration lower than the sensitivity level of the measurement and estimation tools.

A practical sub-optimal solution to these limitations is to control the acetate concentration around a low value A_{ref}, depending on the sensitivity of the measurement devices and the accuracy of the estimation methods.

3. Generic Model Control (GMC)

3.1. GMC background

The Generic Model Control (GMC) is a two-step control approach developed by Lee and Sulivan [31]. In a first step, a feedback linearizing controller is derived (as illustrated in Figure 2) assuming a perfect process knowledge, and allowing the linearization of the nonlinear process behavior. In a second step, the output is forced to track a reference trajectory using a proportional-integral controller. Consider the following single-input single-output (SISO) system:

$$\frac{d}{dt}x = f(x) + g(x)u \tag{10}$$

$$y = h(x) \tag{11}$$

where $x \in \mathbb{R}^n$ is the state vector, $y \in \mathbb{R}^m$ is the process output vector, f and g are nonlinear functions, and h is the measurement function. The time derivative of the output y is given by:

$$\frac{d}{dt}y = \dot{y} = \frac{\partial h}{\partial x}\dot{x} = \frac{\partial h}{\partial x}[f(x) + g(x)u] = L_f h(x) + L_g h(x)u \tag{12}$$

where $L_\bullet h(x) = \frac{\partial h}{\partial x} \bullet (x)$ is the Lie derivative of h along $\bullet$. If $L_{\mathrm{g}}h(\mathrm{x}) \neq 0$ the following input:

$$u = \frac{1}{L_{\mathrm{g}}h(x)}\left(-L_{\mathrm{f}}h(x) + \hat{u}\right) \tag{13}$$

leads to a linear relation between y and the fictive input $\hat{u}$ (i.e. $\dot{y} = \hat{u}$) [32]. The equivalent linear model is then coupled to a proportional integral (PI) controller of the form:

$$\hat{u} = \lambda_1(y_{ref}(t) - y(t)) + \lambda_2 \int_0^t (y_{ref}(\tau) - y(\tau))\partial\tau \tag{14}$$

where y_{ref} is the reference, and λ_1 and λ_2 are the controller parameters chosen accordingly to the desired closed-loop system behavior. The integral action role is to account for model uncertainties, nonlinearities, and disturbances.

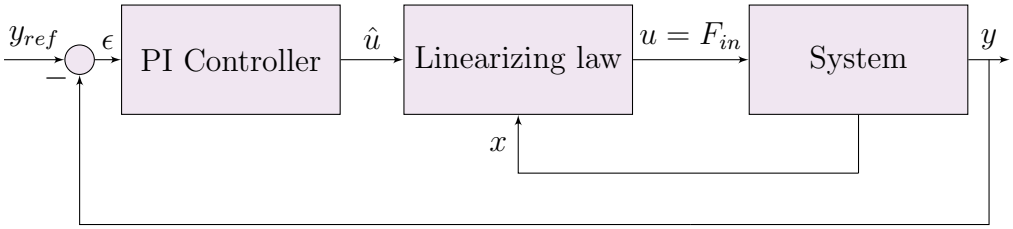

Figure 2: Generic model control scheme

The nonlinear closed-loop stability and the performance analysis of the GMC algorithm are detailed in [33]. Robust stability is ensured for any positive values of λ_1 and λ_2. The proof is based on finding a strict Lyapunov function for the nominal process model and on applying a perturbation theorem. Another stability proof for a similar control structure with kinetic parameter estimation using the Kalman filter is given in [17].

3.2. Application of GMC to E. coli cultures

GMC is applied to an *E. coli* culture as illustrated in Figure 3. Considering acetate concentration as the controlled output, and assuming its availability for measurement ($y = A$).

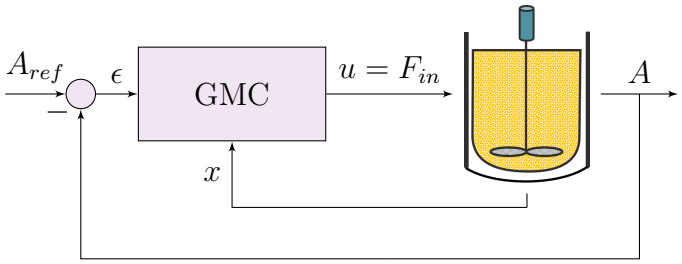

Figure 3: Generic model control applied to fed-batch *E. coli* cultures

As the theoretical value of S_{crit} is very small (below 0.1 g/L) and assuming a quasi-steady state of S (i.e. no accumulation of glucose in the neighborhood of the optimal operating conditions), the small quantity of substrate VS is almost instantaneously consumed by the cells ($\frac{d(VS)}{dt} \approx 0$ and $S \approx 0$), and Equation (4b) yields:

$$\mu_2 X = -\mu_1 X + DS_{in} \tag{15}$$

where μ_1 and μ_2 are nonlinear functions of S, A and O as given by equations (2) and (3). Replacing $\mu_2 X$ by Equation (15), the mass balance equation of A (Equation (4c)) can be expressed as:

$$\dot{A} = -k_{A2}\mu_1 X - \mu_3 X - u\,(A - k_{A2}S_{in}) \tag{16}$$

where $u = D = \frac{F_{in}}{V}$ is the control input. Applying the GMC scheme yields:

$$\dot{A} = \hat{u} = \lambda_1(A_{ref} - A) + \lambda_2 \int_0^t (A_{ref} - A)\partial\tau \tag{17}$$

Equating (16) and (17), the following control law is obtained:

$$F_{in} = V\frac{\hat{u} + (k_{A2}\mu_1 + \mu_3)\,X}{k_{A2}S_{in} - A} \tag{18}$$

$$\hat{u} = \lambda_1(A_{ref} - A) + \lambda_2 \int_0^t (A_{ref} - A)\partial\tau \tag{19}$$

where $(k_{A2}\mu_1 + \mu_3)$ is an assumed uncertain kinetic term. The next section therefore explores a robust control design in order to compensate this uncertainty.

4. Robust control design

The linearizing control law obtained in the previous section can be written in the following form:

$$\begin{aligned} F_{in} &= V\frac{\hat{u} + \theta X}{k_{A2}S_{in} - A} \\ \hat{u} &= \lambda_1(A_{ref} - A) + \lambda_2 \int_0^t (A_{ref} - A)\partial\tau \end{aligned} \tag{20}$$

where θ is the kinetic term given by:

$$\theta = k_{A2}\mu_1 + \mu_3 \tag{21}$$

Structural and parametric uncertainties as well as estimation errors can be lumped into a global parametric error:

$$\delta = \bar{\theta} - \theta \tag{22}$$

where δ is a nonlinear function of (S, A, O) representing possible inexact cancellations of nonlinear terms due to model uncertainties, and $\bar{\theta}$ represents the hypothetical exact (unknown) value. Rewriting the control law in Equation (20) using the new expression of the kinetic term from Equation (22), we obtain:

$$F_{in} = V\frac{\hat{u} + \bar{\theta}X - \delta X}{k_{A2}S_{in} - A} \tag{23}$$

which corresponds to the perturbed reference system:

$$\dot{A} = \hat{u} - \delta X \tag{24}$$

Following a similar approach to the one developed in [14], the time-varying parameter δ is assumed bounded and belonging to the set Δ defined by:

$$\Delta := \{\delta : \underline{\delta} \leq \delta \leq \bar{\delta}\} \tag{25}$$

with $\underline{\delta}$ and $\bar{\delta}$ respectively representing the minimal and maximal values of the assumed bounded polytope set.

The control parameters λ_1 and λ_2 are designed to ensure some robustness and tracking performance to the overall closed-loop system. To this end, the acetate tracking error ($\tilde{A}_1 = A_{ref} - A$) dynamics can be modeled by the following augmented system, illustrated in Figure 4:

$$\begin{aligned} \dot{\tilde{A}}_1 &= \frac{d}{dt}(A_{ref} - A) = -\hat{u} + \delta X \\ \dot{\tilde{A}}_2 &= A_{ref} - A = \tilde{A}_1 \end{aligned} \tag{26}$$

Considering the state vector $x = \tilde{A} = \begin{bmatrix} \tilde{A}_1 & \tilde{A}_2 \end{bmatrix}^T \in \mathbb{R}^n$, the performance output $e = \tilde{A}_1 = (A_{ref} - A) \in \mathbb{R}^{n_e}$ and the disturbance $w = [X \ A_{ref}]^T \in \mathbb{R}^{n_w}$, the control problem can be formulated as a state feedback controller ($\hat{u} = Kx$) applied to the augmented system $\mathcal{M}$:

$$\mathcal{M} : \begin{cases} \dot{x} = A_{\mathcal{M}} x + B_w w + B_u \hat{u} \\ e = C_e x + D_{ew} w + D_{eu} \hat{u} \end{cases} \tag{27}$$

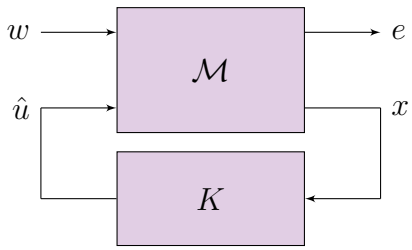

Figure 4: Robust control scheme

The state-space matrices are given by:

$$\begin{aligned} A_{\mathcal{M}} &= \begin{bmatrix} 0 & 0 \\ 1 & 0 \end{bmatrix} \quad B_w = \begin{bmatrix} \delta & 0 \\ 0 & 0 \end{bmatrix} \quad B_u = \begin{bmatrix} -1 \\ 0 \end{bmatrix} \\ C_e &= [1 \ 0] \qquad D_{ew} = [0 \ 0] \qquad D_{eu} = 0 \end{aligned} \tag{28}$$

and the representation of the closed-loop system is therefore given by:

$$\left[\begin{array}{c} \dot{x} \\ e \end{array}\right] = \left[\begin{array}{c|c} A_f & B_f \\ \hline C_f & D_f \end{array}\right] \left[\begin{array}{c} x \\ w \end{array}\right] = \left[\begin{array}{c|c} A_{\mathcal{M}} + B_u K & B_w \\ \hline C_e + D_{eu} K & D_{ew} \end{array}\right] \left[\begin{array}{c} x \\ w \end{array}\right] \tag{29}$$

4.1. Robustness constraints

The control design problem consists in determining the controller parameters λ_1 and λ_2 so as to limit the infinity norm of the closed-loop transfer function within a predefined performance index, $(\left\|\boldsymbol{T}(s) = D_f + C_f \left(s\mathbb{I}_n - A_f\right)^{-1} B_f\right\|_\infty < \gamma_\infty)$, where s is the Laplace variable. First, the following assumptions on the plant parameters are considered:

Assumption 1. *The pair $(A_{\mathcal{M}}, B_u)$ and $(A_{\mathcal{M}}, C_e)$ are respectively stabilizable and detectable*

Assumption 2. $D_{yu} = \mathbb{O}_{n_y, n_u}$

Under the previous assumptions, the Bounded Real Lemma [34] for continuous-time systems gives an equivalent $\mathcal{LMI}$ formulation of the control problem:

Lemma 1. *The $\mathcal{H}_\infty$ norm of the continuous-time transfer function $\boldsymbol{T}(s)$ associated to the closed-loop system (29) is strictly smaller than γ_∞ if and only if there exists a symmetric positive definite matrix Q_∞ verifying:*

$$\begin{array}{l} Q_\infty > 0 \\ \left[\begin{array}{ccc} A_f Q_\infty + Q_\infty A_f^T & B_f & Q_\infty C_f^T \\ B_f^T & -\gamma_\infty \mathbb{I}_{n_w} & D_f^T \\ C_f Q_\infty & D_f & -\gamma_\infty \mathbb{I}_{n_e} \end{array}\right] < 0 \end{array} \tag{30}$$

According to the bounded real lemma, the closed-loop system (29) is stable if and only if there exists: $Q_\infty = Q_\infty^T > 0$ verifying:

$$\left[\begin{array}{ccc} AQ_\infty + B_u K Q_\infty + Q_\infty A^T + Q_\infty K^T B_u^T & B_w & Q_\infty C_e^T + Q_\infty K^T D_{eu}^T \\ B_w^T & -\gamma_\infty \mathbb{I}_{n_w} & D_{ew}^T \\ C_e Q_\infty + D_{eu} K Q_\infty & D_{ew} & -\gamma_\infty \mathbb{I}_{n_e} \end{array}\right] < 0 \tag{31}$$

Considering $L = KQ_\infty$, the following $\mathcal{LMI}$ is obtained:

$$\left[\begin{array}{ccc} AQ_\infty + B_u L + Q_\infty A^T + L^T B_u^T & B_w & Q_\infty C_e^T + L^T D_{eu}^T \\ B_u^T & -\gamma_\infty \mathbb{I}_{n_w} & D_{ew}^T \\ C_e Q_\infty + D_{eu} L & D_{ew} & -\gamma_\infty \mathbb{I}_{n_e} \end{array}\right] < 0 \tag{32}$$

and the controller given by $K = LQ_\infty^{-1}$ ensures a level of robustness w.r.t the bounded uncertainty δ. Next, the desired performance constraints are defined and added to the robustness condition (32).

4.2. Performance constraints

Besides ensuring the robustness of the closed-loop, it is desirable to achieve some performance in terms of the transient response (e.g., damping, response time, etc.). In other words, constraints are added to the location of closed-loop poles of system (29).

For a second-order system with poles $\lambda = -\zeta\omega_n \pm j\omega_d$, the step response is characterized by the undamped natural frequency $\omega_n = |\lambda|$, the damping ratio ζ, and the damped natural frequency ω_d. To ensure a desired transient response, specific bounds are imposed on these quantities, thus constraining the closed-loop poles λ in a prescribed region of the complex plane. Pole placement constraints can be expressed using $\mathcal{LMI}$ regions, which are known to have interesting geometric properties for control purposes (convexity, symmetry, ...) [34]. A suitable region satisfying this criterion is the intersection of the half-plane $s < -\alpha < 0$, the disk of radius r and the conic sector defined by an angle Θ. The corresponding region $\mathcal{S}(\alpha, r, \Theta)$ is defined as follows:

$$\mathcal{S}(\alpha, r, \Theta) = \{a < -\alpha < 0, \quad |s = a + jb| < r, \quad \tan\Theta a < -|b|\} \tag{33}$$

In this way, it is possible to set a minimum decay rate α, a minimum damping ratio $\zeta = cos(\Theta)$, and a maximum undamped natural frequency $\omega_d = rsin(\Theta)$ [35].

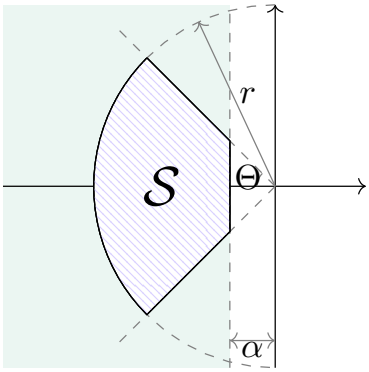

Figure 5: Representation of the region $\mathcal{S}(\alpha, r, \Theta)$

The poles of the closed-loop system (29) are contained in the region $\mathcal{S}(\alpha, r, \Theta)$, if there exists a symmetric positive definite matrix $Q = Q^T$ verifying [34]:

$$\begin{gathered} A_f Q + Q A_f^T + 2\alpha Q < 0 \\ \begin{bmatrix} -rQ & A_f Q \\ Q A_f^T & -rQ \end{bmatrix} < 0 \\ \begin{bmatrix} \sin\Theta\left(A_f Q + Q A_f^T\right) & \cos\Theta\left(A_f Q - Q A_f^T\right) \\ \cos\Theta\left(Q A_f^T - A_f Q\right) & \sin\Theta\left(A_f Q + Q A_f^T\right) \end{bmatrix} < 0 \end{gathered} \tag{34}$$

Our control design problem consists then in finding a state-feedback gain K that:

- guarantees the H_∞ performance $\|\boldsymbol{T}(s)\|_\infty < \gamma_\infty$.
- places the closed-loop poles in the $\mathcal{LMI}$ region $\mathcal{S}(\alpha, r, \Theta)$ defined by Equation (33).

The first criterion (robustness) is ensured by solving Equation (32), and computing the matrix Q_∞. On the other hand, a sufficient condition to ensure the performance constraints given by Equation (34) is to take $Q = Q_\infty$, yielding:

$$\begin{gathered} A_f Q_\infty + Q_\infty A_f^T + 2\alpha Q_\infty < 0 \\ \begin{bmatrix} -rQ_\infty & A_f Q_\infty \\ Q_\infty A_f^T & -rQ_\infty \end{bmatrix} < 0 \\ \begin{bmatrix} \sin\Theta\left(A_f Q_\infty + Q_\infty A_f^T\right) & \cos\Theta\left(A_f Q_\infty - Q_\infty A_f^T\right) \\ \cos\Theta\left(Q_\infty A_f^T - A_f Q_\infty\right) & \sin\Theta\left(A_f Q_\infty + Q_\infty A_f^T\right) \end{bmatrix} < 0 \end{gathered} \tag{35}$$

The robust GMC control design procedure based on $\mathcal{LMI}$s is summarized in the following steps:

- **Step1**: Select a suitable range for the uncertain variable δ.
- **Step2**: Determine the values of α, r, Θ in order to meet a suitable transient performance.
- **Step3**: Solve (off-line) the bounded real lemma (Equation (32)) and the performance $\mathcal{LMI}$ (Equation (35)) simultaneously, to compute the gain K, and obtain the robust GMC controller parameters λ_1 and λ_2.

5. Acetate estimation

The acetate concentration needs to be determined on-line to apply the proposed GMC strategy and drive the system close to the optimal operating conditions. However, no device presenting a sufficient level of accuracy is currently available on the market. This study proposes estimating the acetate and glucose concentrations from the viable biomass concentration signal, which is efficiently measurable with low noise amplitudes via spectrophotometric probes. However, before implementing a state estimation algorithm, the mechanistic model presented in section 2 has to be observable.

Observability is a system property that relates to the possibility of estimating the system state based on the available measurement information. A detailed analysis of the observability of the bioprocess model under consideration is given in [30]. The biomass concentration measurement is sufficient to reconstruct the acetate concentration as long as the substrate concentration remains at a sufficiently low level (0 g/L $< S <$ 0.1 g/L).

Since the bioprocess's observability is guaranteed, acetate concentration can be estimated using a state observer, which can take various forms [36]. In [30], an extended

Kalman filter (EKF) was applied -under specific conditions- to estimate the glucose and acetate concentrations using various sensor configurations. Whereas the EKF was able to reconstruct the acetate concentration from the biomass measurement efficiently, the strong nonlinearities in the kinetic model (4) can lead to significant estimation errors and a low convergence rate EKF based on the linearization of the nonlinear process.

In the present study, the Unscented Kalman Filter (UKF) [37, 38] is considered. Unlike the EKF, the UKF does not involve any linearization around the current state estimate. A set of sample points is propagated through the nonlinear system, which allows the reconstruction of the state estimate's mean and covariance under the assumption of a Gaussian distribution of the noise.

The UKF algorithm implemented in this study is detailed in [39], where it was implemented for a similar overflow mechanistic model for fed-batch cultures of hybridoma cells. Since the biomass measurements are provided in discrete samples of time, the continuous-discrete version of the UKF is implemented, i.e., a continuous-time model prediction and a discrete-time measurement update.

The UKF estimator combined with the robust GMC controller applied to the E. coli culture is illustrated in Figure 6.

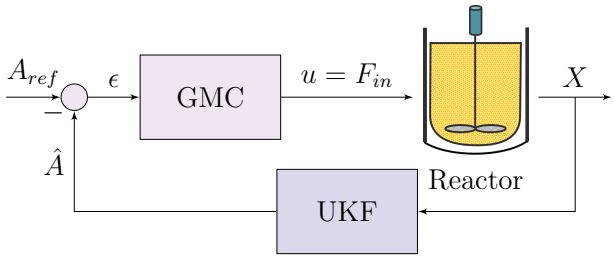

Figure 6: Generic Model Control combined with the Unscented Kalman filter applied to fed-batch *E. coli* cultures

6. Numerical simulations

In this section, several numerical simulations are achieved before the experimental validation. First, the estimation of the acetate concentration using the Unscented Kalman filter is tested. Second, the performance and robustness of GMC are assessed assuming that the acetate concentration is available for measurement. Finally, the estimation and control algorithms are combined. The cultures are achieved in a 5-L bioreactor and the kinetic and stoichiometric parameters are those estimated in a previous work [28].

A predefined feeding profile is applied to the system, consisting of a batch phase followed by a fed-batch phase with an exponential feeding profile. The UKF tuning parameters (α, β, κ), the process and measurement noise covariance matrices Q and R, and the initial state covariance matrix P_0 are given in Table 1.

Table 1: UKF covariance matrices, sigma point tuning parameters, and initial conditions

Parameter	Value	Unit
Q	$diag[10^{-4}, 10^{-2}, 10^{-2}, 10^{-8}]$	g/L
R	10^{-4}	g/L
P_0	$10^{-4} \times \text{eye}(N)$	g/L
$[\alpha,\, \beta,\, \kappa]$	[1, 2, 0]	-
X_0	0.1	g/L
S_0	5	g/L
A_0	0.1	g/L
V_0	3.5	L
S_{in}	500	g/L

The convergence of the UKF is first tested with (largely) erroneous initial conditions. Figure 7 shows the performance of the UKF in estimating glucose and acetate concentrations based on the biomass concentration measurement affected by additive white noise with zero mean and a standard deviation of 0.1 g/L. After a transient phase of 3 h, both states are well estimated and the convergence is achieved. The mean square errors of the substrate and acetate estimates during this test are: $\overline{e_S} = 0.53$ g/L and $\overline{e_A} = 0.23$ g/L respectively, which include the initial transient phase but are coherent with the sensitivity of the measurements and the noise levels (0.1 g/L).

Further, the performance of the robust GMC design based on the $\mathcal{LMI}$ approach with the regional pole assignment is tested. The control objective is to regulate the acetate setpoint A_{ref}, chosen sufficiently low to approach the neighborhood of the optimal trajectory but also sufficiently high to stay within the limit of the observation sensitivity (0.1 g/L) and maintain the culture in respiro-fermentative mode. The acetate concentration is assumed available on-line for feedback, with the consideration of measurement noise.

The first step in our design approach is to define upper and lower bounds for the parametric uncertainty δ. The expression of the kinetic parameter θ is given by:

$$\theta = k_{A2}\mu_1 + \mu_3 \tag{36}$$

The expression of the uncertain term θ, and the kinetic terms μ_1 and μ_3 contain the parameters $k_{A2}, K_s, K_{iA}, k_{OS}, K_A$. These parameters can deviate from their nominal values, thereby deviations of maximum 15% are considered. Consequently, the range Δ can be defined by $\underline{\delta} = 0$ and $\bar{\delta} = 0.1$.

Regarding the performance constraints, we desire to enforce a maximal settling time $T_s = \frac{4}{\zeta\omega_n} = \frac{4}{\alpha}$ equal to 2 h, and to prevent fast controller dynamics.

To this end, we characterize the section $\mathcal{S}(\alpha, r, \theta)$ as the intersection of the half-plane $x < -\alpha = -\frac{4}{T_s}$ with the disk of radius $r = 4$ centred at the origin, and the conic section defined by $\Theta = \frac{\pi}{2}$ rad.

In light of these constraints, the $\mathcal{LMI}s$ (Equations (32) and (35)) are solved numer-

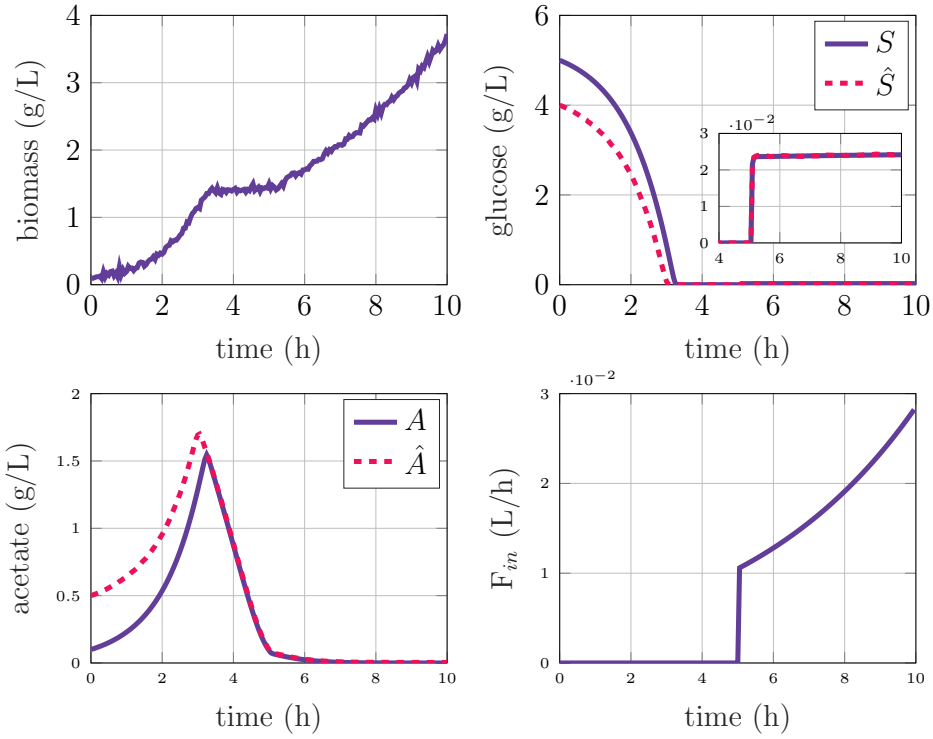

Figure 7: Convergence of UKF starting from erroneous initial conditions - estimation of glucose and acetate concentrations based on biomass concentration measurements.

ically using the solver *SeDuMi* [40] and the following results are obtained:

$$Q_\infty = \begin{bmatrix} 0.143 & -0.034 \\ -0.034 & 0.015 \end{bmatrix} \qquad \lambda = \begin{bmatrix} \lambda_1 = 5.61 \\ \lambda_2 = 9.55 \end{bmatrix} \tag{37}$$

corresponding to the following damping ratio and natural frequency:

$$\zeta = 0.91 \qquad \omega_n = 3.09 \ \text{rad/h} \tag{38}$$

satisfying the performance constraints regarding the settling time $T_s = \frac{4}{\zeta \omega_n} = 1.43$ h.

Figures 8 and 9 show the closed-loop response of biomass, substrate, acetate concentrations, and the corresponding feed flow-rate in 50 different runs, with $A_{ref} = 0.5$ g/L and kinetic parameter deviations. A white noise is added to the acetate concentration measurement with zero mean and a standard deviation of 0.1 g/L. In all the runs, biomass follows a similar exponential growth in the first hours, while the model errors show their effect in the final hours. Nevertheless, the model uncertainties have a minor influence on the controller performance as can be observed in the acetate evolution, where the set-point is regulated and robust convergence is achieved by the controller. The noisy acetate

signal has a mean value of 0.49 g/L and the tracking error ($A_{ref} - A$) has a RMSE of 0.0314 g/L which is lower than the measurement noise amplitude (0.1 g/L). Note that the maximal 2h settling time condition is also satisfied. The biomass productivity remains higher than 90 % of the nominal value in 90% of the runs, which is satisfactory from an operational point of view.

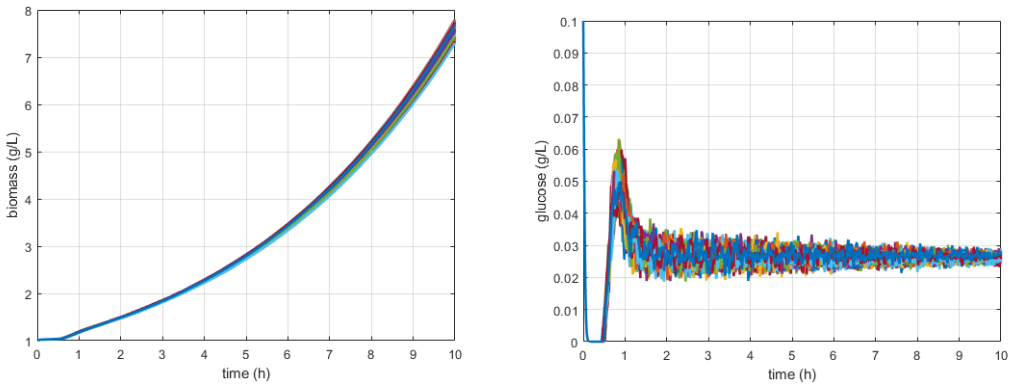

Figure 8: Biomass and substrate concentrations in 50 runs with kinetic parameter deviations (up to 15%) and a measurement noise standard deviation of 0.1 g/L using the robust GMC control strategy.

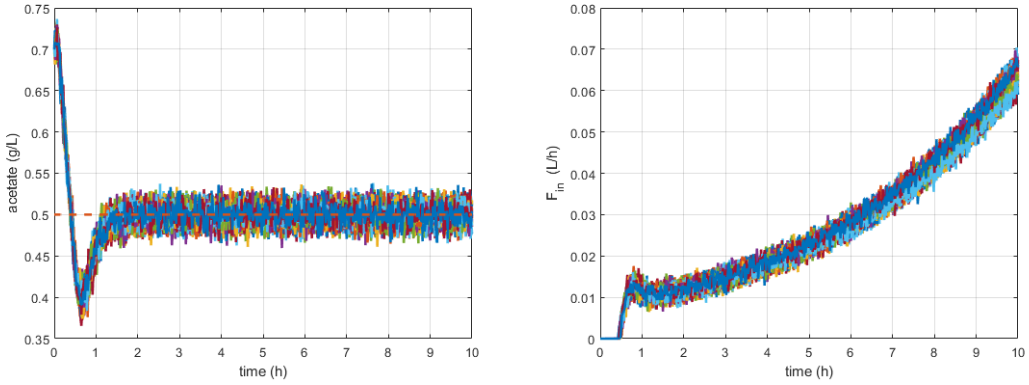

Figure 9: Acetate concentration and feed flow-rate in 50 runs with kinetic parameter deviations (up to 15%) and a measurement noise standard deviation of 0.1 g/L using the robust GMC control strategy.

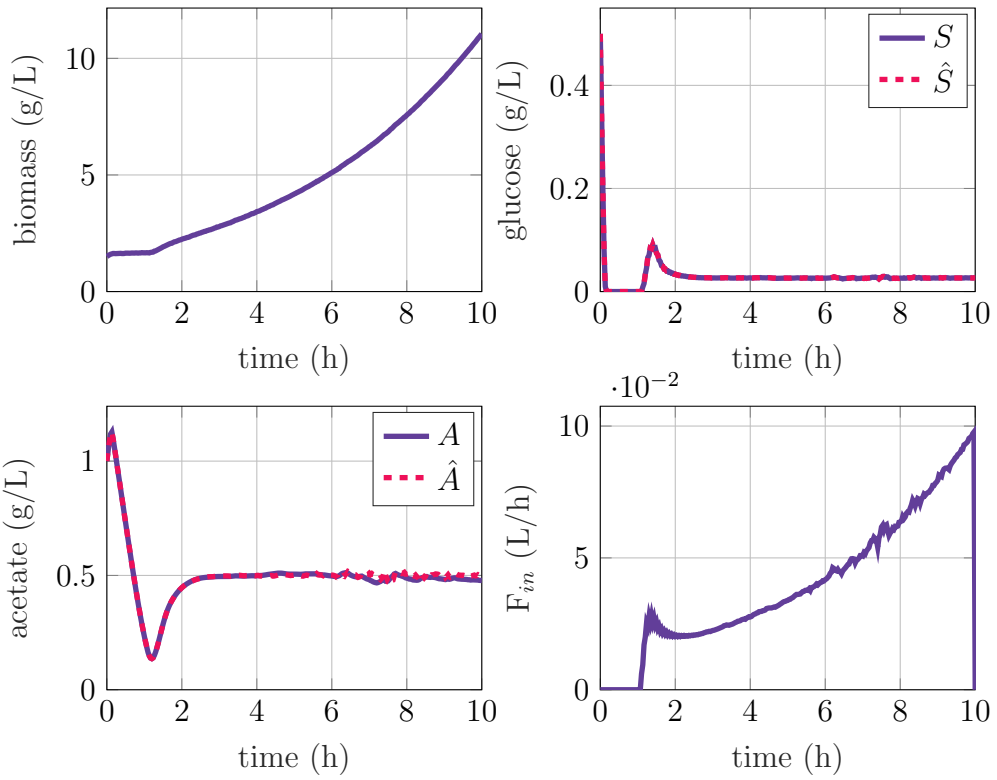

Figure 10: Coupled UKF-GMC with random parameter values (±15% variation) and a white measurement noise (std =0.1 g/L)).

Finally, the UKF and robust GMC are coupled, and their overall performance assessed in a new set of numerical simulations. The UKF initial conditions are selected randomly with a maximum deviation of 20% from the real values. Kinetic parameter variations of ±15% of the nominal values and a white measurement noise with a standard deviation of 0.1 g/L are considered. As shown in Figure 10, the UKF behaves very well and converges in the first hours to the real state trajectories. We can observe small estimation errors with peaks and troughs around the real substrate value when the substrate (glucose) concentration reaches a critical level of S_{crit}. Fortunately, this is not too detrimental for the controller which is still able to track the acetate concentration reference set-point.

In order to test further the performance and robustness of the control approach, a comparison is achieved with the classical GMC algorithm presented in [22]. The parameter tuning is performed by selecting a desired rise time. In the presented simulations the following parametrization is chosen:

$$\xi = 1, \quad t_r = 2 \text{ h}, \quad \lambda_1 = 3, \quad \lambda_2 = 2.25$$

The classical and the robust controllers are tested in the ideal model case (no parameter variation), and in the case of a random variation in all model parameters up to 30%

of their nominal value. A series of 100 Monte Carlo (MC) simulations is performed and the results are summarized in Table 2.

The results of one simulation are shown in Figure 11, where both approaches perform similarly in the ideal model case. However, we can see that with increasing levels of parameter variation, the robust GMC performs better in terms of reference tracking. The mean square errors ($\overline{e_A}$) and the mean acetate concentration ($\overline{A}$) show that the robust tuning of the parameters allows the controller to achieve the control objective accurately. We can also observe that a 30% variation is the breakpoint of both methods, with a slight advantage to the robust GMC design.

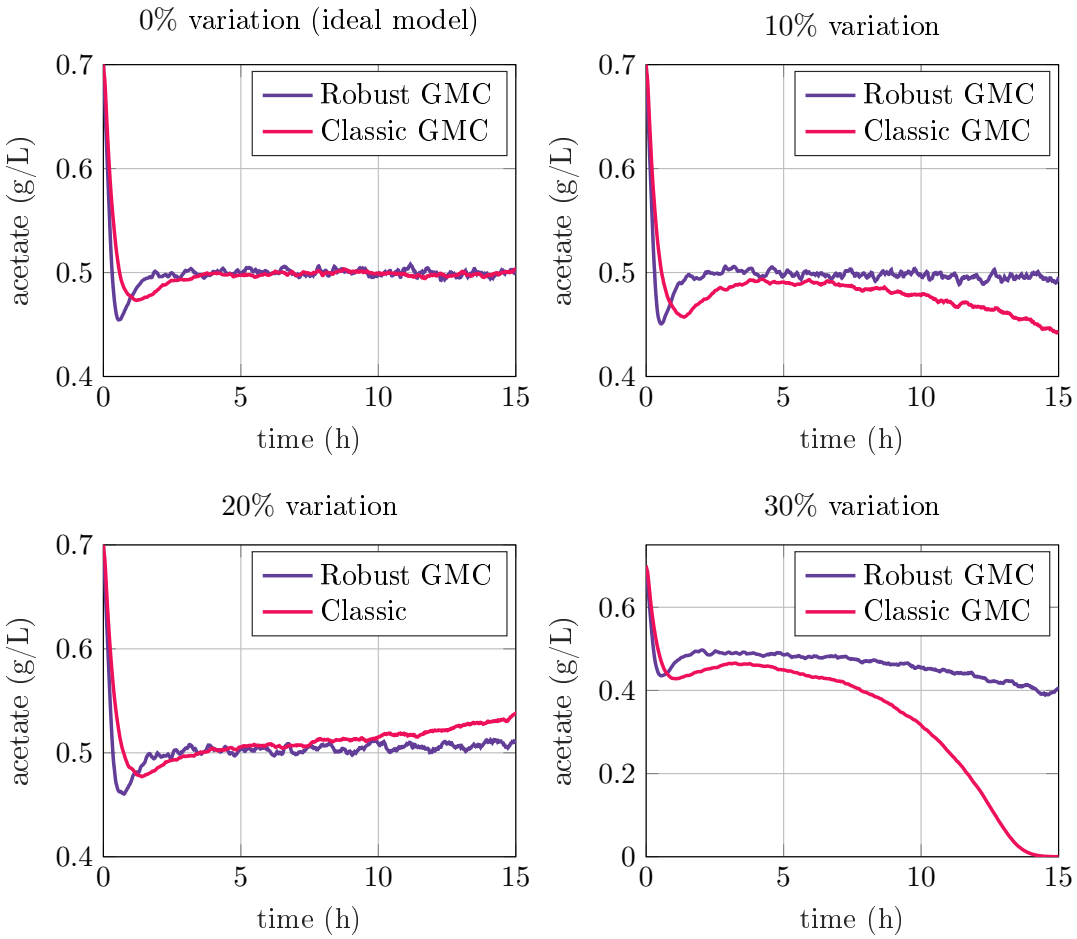

Figure 11: Comparison between the classical and robust tuning of the GMC strategy, with increasing levels of parameter variation.

Table 2: Results of 100 Monte Carlo simulations comparing the classical and robust GMC strategies

	$\overline{A}$ (Classic)	$\overline{A}$ (Robust)	$\overline{e_A}$ (Classic)	$\overline{e_A}$ (Robust)
0%	0.4996	0.4996	0.0226	0.0192
10%	0.4968	0.4989	0.02	0.0293
15%	0.5009	0.5001	0.0343	0.0207
20%	0.4992	0.4998	0.0456	0.0224
25%	0.4885	0.4974	0.0643	0.0261
30%	0.4744	0.4944	0.0843	0.0294
35%	0.4741	0.4913	0.0889	0.0418

7. Materials and methods

This section describes the strain, materials, growth media, and preparation methods utilized in the experiments.

7.1. Microbial strain

The *E. coli* BL21(DE3) strain was used for all fermentations. BL21 is known to lead to a low acetate formation compared to *E. coli* K12, which is suitable for high cell density cultivations, as well as lower sensitivity to varying growth conditions [41].

7.2. Growth media and culture conditions

The media were prepared according to the protocol cited in [10, 23]. The media used during the different stages of the cultures are the Lysogeny broth medium (LB) and a defined high-density fermentation medium (HDF) [23]. Their respective compositions for the batch (precultures & bioreactor) and fed-batch cultures are given in Tables 3 and 4. During the preparation, solutions were filtered and sterilized in autoclave to avoid contamination.

Table 3: Composition of the LB media used during preparations

Component	**Concentration** (g/L)
Peptone	10
Yeast extract	5
NaCl	6

Table 4: Composition of the defined HDF media

Components	**Batch medium** (./L)	**Feeding solution** (./L)
Glucose	5 g	500.0 g
KH_2PO_4	13.3 g	–
$(NH_4)_2 HPO_4$	4.0 g	–
$MgSO_4 \cdot 7H_2O$	1.2 g	20.0 g
Citric acid	1.7 g	–
EDTA	8.4 mg	13.0 mg
$CoCl_2 \cdot 6H_2O$	2.5 mg	4.0 mg
$MnCl_2 \cdot 4H_2O$	15.0 mg	23.5 mg
$CuCl_2 \cdot 4H_2O$	1.5 mg	2.5 mg
H_3BO_3	3.0 mg	5.0 mg
$Na_2MoO_4 \cdot 2H_2O$	2.5 mg	4.0 mg
$Zn\,(CH_3COO)_2 \cdot 2H_2O$	13.0 mg	16.0 mg
Fe^{III}Citrate	100.0 mg	40.0 mg
Thiamine ·HCl	4.5 mg	–

7.3. Reactor setup

The cultivations were performed in a bioreactor consisting of a 5L jacketed glass vessel and a digital control unit or *DCU* (BIOSTAT B plus, Sartorius Stedim Biotech, Germany). The reactor is equipped with a water jacket and an agitation motor.

The monitoring of the cultures is possible thanks to a potentiometric pH sensor (Hamilton, Switzerland), optical dissolved oxygen (DO) probe (Hamilton, Switzerland), and a temperature sensor (Sartorius, Germany). Also, biomass concentration is available on-line via an absorption-based photometric turbidity probe (Fundalux II, Sartorius, Germany).

7.4. Analytical Methods

During the fermentation, samples were taken every hour. The optical density (OD) of the samples was measured at 600 nm in a UV spectrophotometer (Shimadzu, Pharmacia Biotech, USA). Samples were diluted with deionized water to obtain OD in the linear range (0-0.3 OD), and then correlated with dry cell weight (DCW) using a calibration curve to obtain the off-line biomass concentration. To determine dry cell weights (DCW), 10 mL aliquots of culture medium were filtered and placed in pre-weighed polystyrene micro weighing dishes, dried at 65°C for 24 h until constant weight, and weighed (1 OD = 0.39 g/L).

Samples were centrifuged and the supernatant was decanted and then stored at -8 °C. Glucose concentration was measured using the Dinitro Salicylic Acid (DNS) Method.

Acetate determination was performed using an enzymatic acetic acid test kit (Megazyme, Ireland). The sensitivity level of analytical methods is estimated around 0.1 g/L [30].

7.5. Operating conditions

The batch and fed-batch fermentations were conducted under controlled conditions. The pH is regulated at 7 by adding solutions of 12.5% ammonium hydroxide (base) or phosphoric acid 0.5 M (acid). Dissolved oxygen (pO_2) was maintained above 30% air saturation by a two-level controller, increasing the agitation rate when the oxygen demand of the cells increases. When the maximal agitation rate is reached, the airflow is increased. Minimum values for airflow and agitation were imposed (1 L/min and 200 rpm, respectively).

The temperature was controlled by the DCU at 37 °C using a heating water jacket.

7.6. Pre-cultures

The cryogenic culture was incubated for 24h on LB-agar Petri dishes at 37°C. Primary inocula consisting of Lysogeny broth (LB) media (Table 3), and one colony of *E. coli* were prepared in 150-mL Erlenmeyer shake flasks (50 mL working volume) and grown 8h at 37°C in an air shaker at 250 rpm.

To adapt cell populations to fermentor conditions, shake flasks containing the HDF media (Table 4) (250 mL) were inoculated from the LB media cultures (5% v/v) and incubated overnight (14-16h) at 37°C in the air shaker at 200 rpm.

7.7. Batch and fed-Batch cultures

All fermentations were carried in batch, followed by a fed-batch phase. Initial batch cultures of $V = 3.5$ L were pre-equilibrated to the appropriate operating conditions (pH, pO_2 temperature) before inoculation with 5% v/v seed culture, where the initial OD_{600} in the fermentor reaches 0.3-0.6. It is noteworthy that a lower initial volume was not possible, since the biomass probe would not be completely immersed. Sterile filtered anti-foam was added via a peristaltic pump when necessary throughout the cultivations.

The batch phase was monitored during the day. Once the glucose was nearly depleted, the fed-batch phase started, and the feeding solution was added with a rate determined by the controller, and applied by a Reglo-digital peristaltic pump (Ismatec, Germany).

7.8. Culture monitoring and control

The measurements provided by the DCU (pH, pO_2, Temperature ...) were monitored in real-time by the MFCS software (Sartorius, Germany). The control and estimation algorithms were coded in Matlab for simulations and implemented on-line in LabView using shared-library and MathScript nodes. Measurements provided by MFCS were imported to LabView by shared libraries. The biomass signal was measured separately by a data acquisition device from national instruments (NI USB-6000USB Multifunction

DAQ Device, National Instruments, USA) and squired in LabView using DAQMax library. Figure 12 shows a diagram of the different devices used for online implementation.

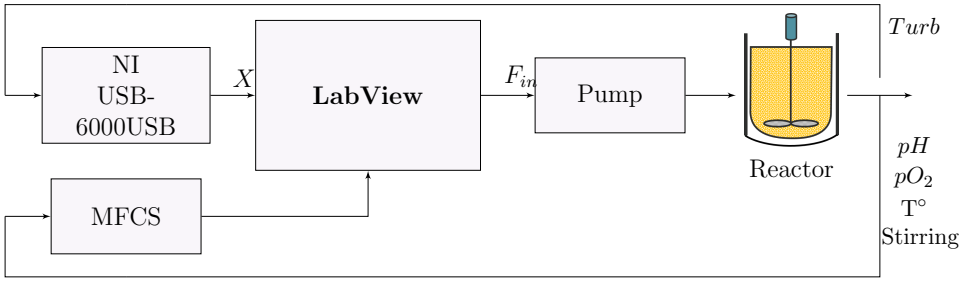

Figure 12: Real-time implementation diagram

8. Experimental results and discussion

Two control experiments were performed to test the tracking performance and robustness of the developed UKF-GMC strategy in a real-time environment. Each experiment consisted of a batch phase followed by a fed-batch phase (control phase). The evolution of the measured biomass (on-line & off-line), glucose, acetate concentrations (off-line), and their estimates, as well as the feed flow-rate (controller output), are shown in Figures 13 and 15. The operating conditions are also illustrated in Figures 14 and 16.

8.1. Culture evolution

After reaching the desired operating conditions, the reactor is inoculated with the seed culture, and the batch phase begins. As shown in Figures 13 and 15, the initial biomass concentration in the reactor ranges from 0.1-0.2 g/L. During this phase, the biomass follows an exponential growth and reaches up to 2 g/L. Since glucose consumption leads to acetate production, the culture is in respiro-fermentative mode.

The batch phase ends after 4-5 h, after the almost complete consumption of the glucose in the medium. On-line indicators of the glucose depletion are the sudden decrease of the stirring speed due to the decrease of cell demand for oxygen, the sudden increase of the pH combined with the decrease of injected base volume (see Figures 14 and 16). Note that the estimation algorithm is launched during the batch phase. The initial conditions, control parameters, and acetate references for each experiment, as well as the values for the measurement and process noise covariance matrices are given in Table 5,.

The fed-batch phase starts right after the first on-line flags and preferably before complete depletion of glucose, to avoid the switch to the respirative mode. The GMC controller is launched after setting up the acetate reference and the control parameters. The feed solution is injected and the cells resume their growth, resulting in an increase of the stirring speed due to the glucose oxidation, and the decrease of pH due to CO_2 emission which requires base addition to maintain the pH around its set-point. The

fed-batch phase continues until reaching the saturation limit of the turbidimetric probe (around 7-8 g/L). The maximum attainable cell density depends on the oxygenation limitation related to the bioreactor scale as can be observed in several studies [10, 28, 42]. Therefore the end of the fed-batch phase is forced by either an exhausted feed medium, or the limiting oxygenation conditions.

Table 5: Control & estimation parameters and initial conditions used in the experiments

	Experiment 1	**Experiment 2**
Sampling time	$t_e = 0.05\ h$	$t_e = 0.05\ h$
Acetate reference	$A_{ref} = 0.5$ g/L	$A_{ref} = 0.7$ g/L
Q	$diag[10^{-4}, 10^{-2}, 10^{-2}, 10^{-8}]$ g/L	$diag[10^{-4}, 10^{-2}, 10^{-2}, 10^{-8}]$ g/L
R	10^{-4} g/L	10^{-4} g/L

8.2. Acetate and glucose estimation

As presented in the simulation section, the on-line biomass concentration measurement provided by the turbidimetric probe, and the kinetic model with identified parameter values from [28] are used to estimate the acetate and glucose concentrations using the UKF. The estimation is launched during the batch phase (around 4h).

The measurement noise affecting the biomass concentration signal is considered as a centered white noise with a standard deviation of 0.1 g/L. On the other hand, the degree of confidence in the model regarding the substrate and acetate concentration signals is lower compared to the biomass concentration.

In both experiments, the UKF performance in the fed-batch phase is satisfactory, despite the initialization errors and the model uncertainties. The glucose and acetate estimations fit very well with the off-line measurements, and the convergence is achieved in less than 1 h. Table 6 shows the estimation mean square error values for each estimated state (i.e., substrate and acetate) during the fed-batch phase of both experiments, which are lower than the measurement sensitivity (0.1 g/L).

Table 6: Experimental study - UKF estimation mean square errors (in g/L)

	$\overline{e_S}$(g/L)	$\overline{e_A}$(g/L)
Experiment 1	0.0885	0.0679
Experiment 2	0.0381	0.1132

8.3. GMC control performance

The control objective, as explained in previous sections, is to regulate the acetate concentration to a predefined set-point, and maintain the culture in the respiro-fermentative

mode close to the optimal limit. As can be seen in Figures 13 and 15, acetate accumulation is avoided in both cultures, and the concentration is limited to less than (1 g/L) during the fed-batch phase.

In the first experiment (Figure 13), the estimated acetate concentration is regulated and converges to the desired reference, respecting the chosen settling time. The second experiment (Figure 15) presents the same performance regarding the GMC algorithm convergence, with a different set-point and a longer control time.

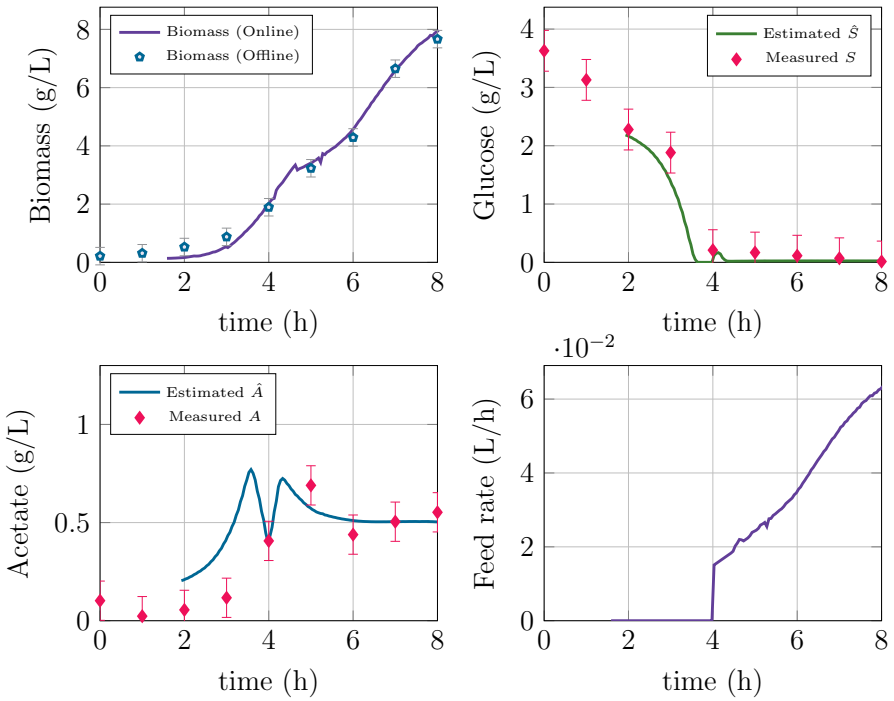

Figure 13: Experiment 1: Time evolution of the measured biomass, glucose, acetate concentrations estimates, and feed-rate

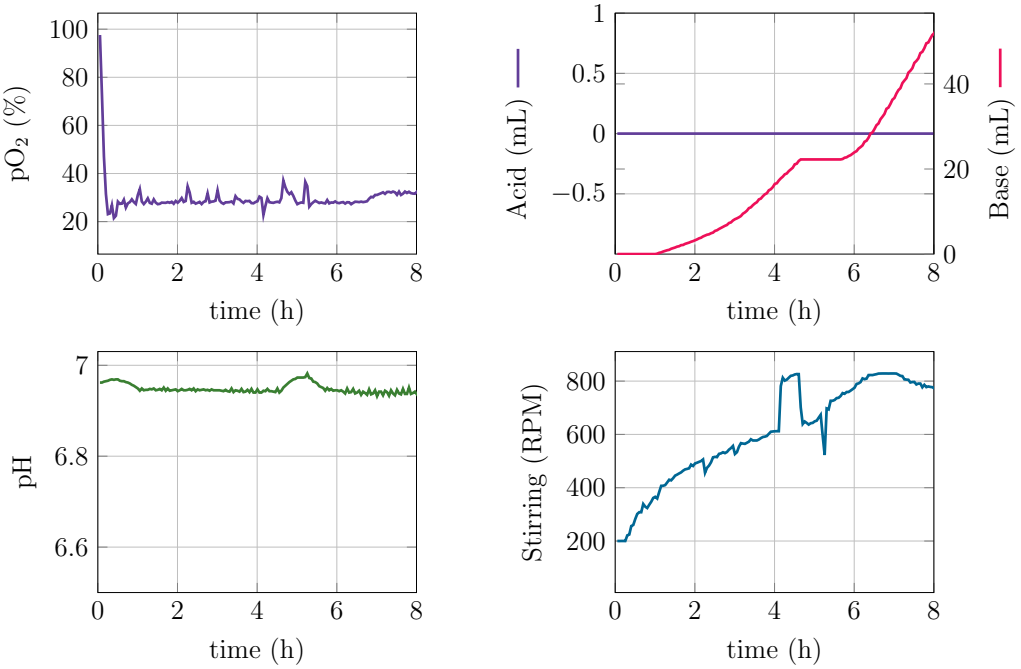

Figure 14: Experiment 1: Time evolution of the pO_2, acid and base concentrations, pH and stirring

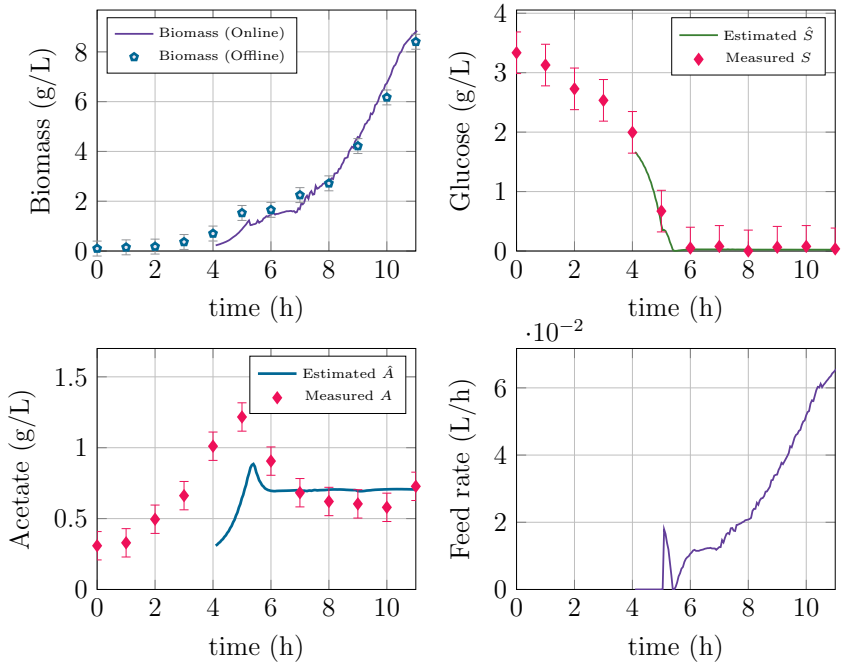

Figure 15: Experiment 2: Time evolution of the measured biomass, glucose, acetate concentrations, and feed-rate

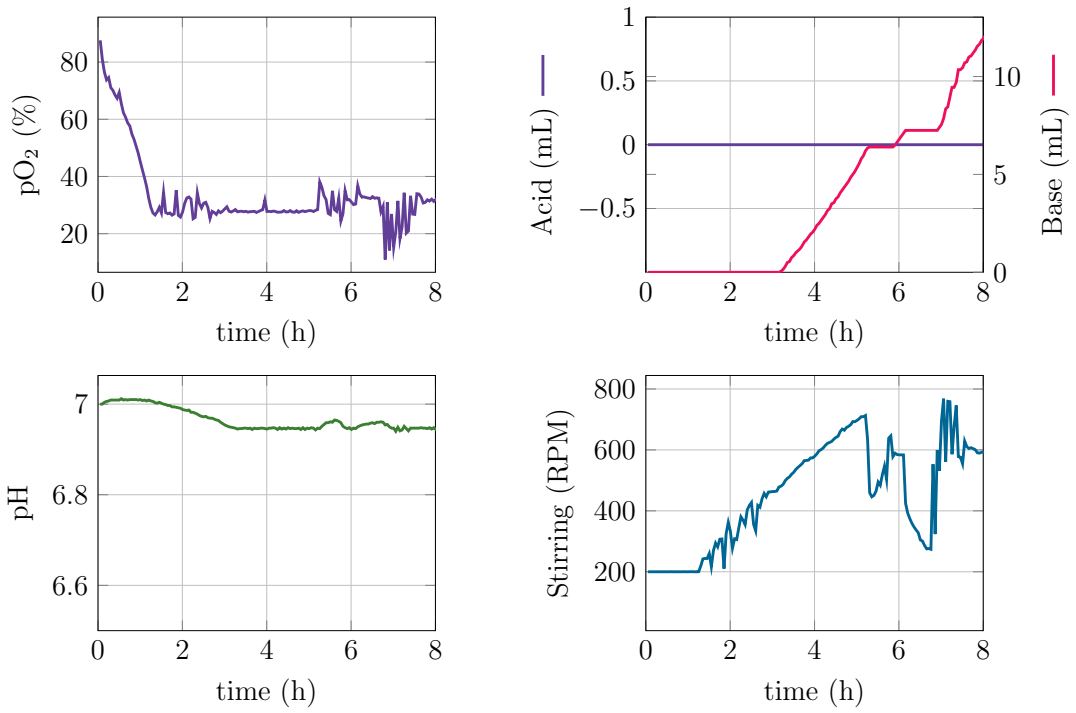

Figure 16: Experiment 2: Time evolution of the pO_2, acid and base concentrations, pH and stirring

8.4. Discussion

The presented control method provides a practical approach to avoid overflow metabolism in *E. coli* fed-batch cultures. However, it offers a suboptimal solution, since accurate online measurements of the substrate concentration at the critical level are impractical.

In order to evaluate the efficiency of the proposed approach, a comparison is performed with another suboptimal regulation strategy. In this approach, the growth rate is regulated to a set reference value μ_{set}, usually chosen slightly below the maximal growth rate in order to avoid acetate accumulation while maximizing the biomass productivity. This control objective is attained by tracking a predefined biomass trajectory corresponding to the chosen reference growth rate [43, 44].

In this study, we compare the robust acetate regulation to an adaptive GMC strategy tracking a defined growth rate presented in [19]. For this purpose, we set the biomass regulation to track a defined growth rate μ_{set} chosen at 90% of the theoretical maximal value ($\mu_{max} = 0.26$ L/h), corresponding to the critical substrate concentration and the maximal oxidative capacity. On the other hand, we set the acetate regulation to track a reference of 0.5 g/L.

First, we assume that the model parameters and maximal growth rate $\mu_{X_{max}}$ are perfectly known. Then, we introduce a fixed variation in the maximal oxidative capacity q_{Omax}, leading to a variation in the maximal growth rate.

Simulation results are shown in Figures 17 and 18. In the ideal model case (no parameter variation), the biomass growth regulation (GMC-X) has a slightly better overall performance. The reference growth rate is tracked accurately at 0.23 h^{-1} corresponding to 89% of its maximal value. On the other hand, regulating the acetate concentration (GMC-A) at 0.5 L/h leads to a biomass growth rate of 0.21 h^{-1} corresponding to 81% of the maximal value as can be seen in Table 7. This result shows that the presence of acetate in the medium reduces the biomass growth rate, due to lower substrate consumption rate caused by the activation of the acetate consumption pathways according to the bottleneck theory. However, keeping the acetate at a low concentration reduces its inhibitory effect, and keeps the culture close to the optimal conditions.

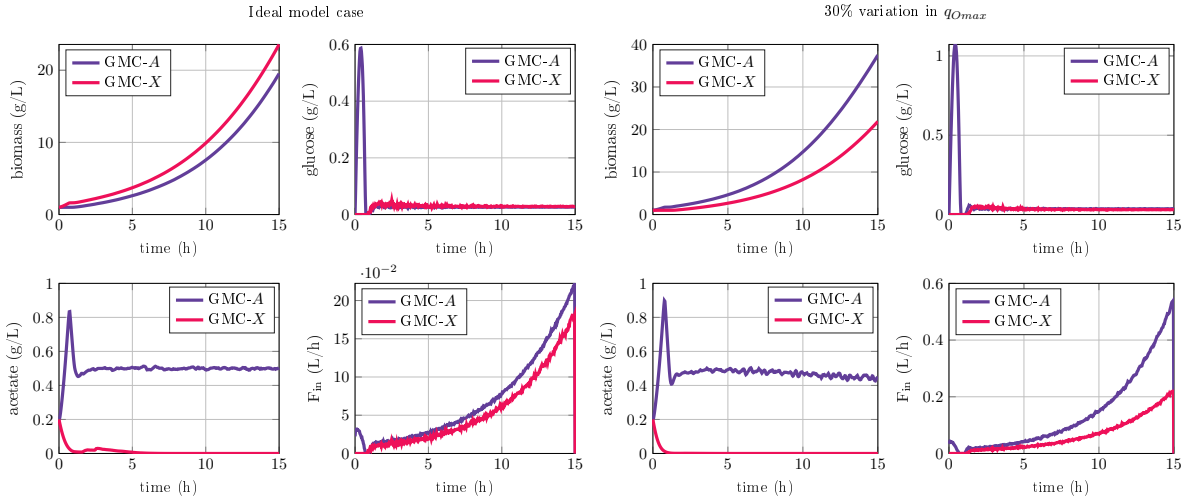

Figure 17: Comparison between the control approaches in the ideal model case, and in the presence of parametric variation. Plot of the state variables and the feed-rate.

Table 7: The effect of parameter variation on the control performance

Variation in q_{Omax}	$\frac{\mu_X}{\mu_{max}}$% (GMC-X)	$\frac{\mu_X}{\mu_{max}}$% (GMC-A)	S_{crit}
0%	89%	81%	0.0375
10%	81%	85%	0.046
20%	75%	89%	0.0529
30%	70%	93%	0.0628

The introduction of a 20% variation in q_{Omax} leads to an increase of the critical substrate concentration S_{crit} and consequently the maximal growth rate μ_{max}.

Despite the model mismatch, the biomass growth rate regulation presents a good performance in tracking the reference rate. However, it corresponds to only 75% of the

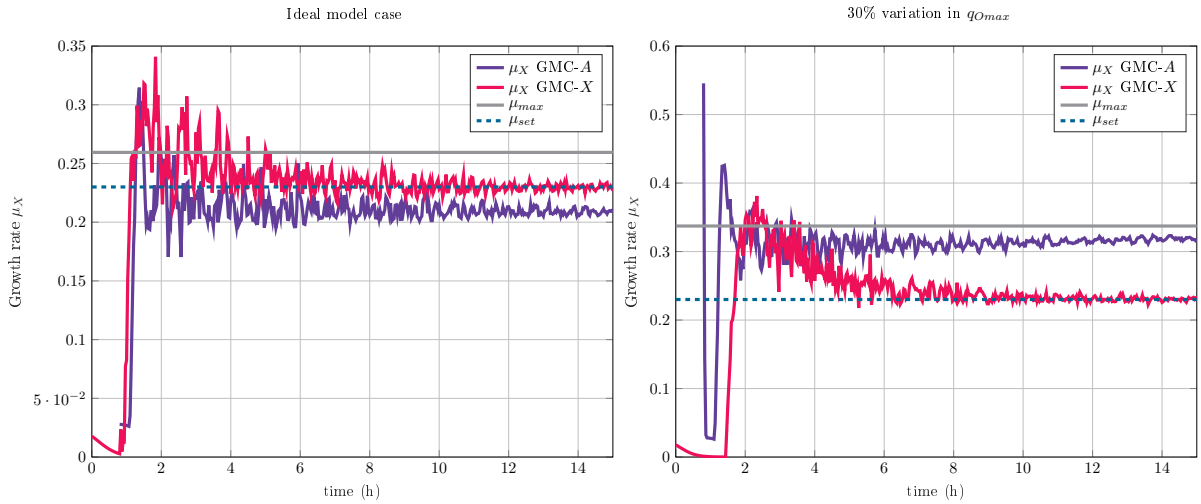

Figure 18: Comparison between the control approaches in the ideal model case, and in the presence of parametric variation. Plot of the specific biomass growth rates.

new maximal value, and therefore the biomass productivity is also lower than its optimal value compared to the nominal case. The acetate regulation on the other hand offers a more consistent performance, and gives a better growth rate ratio (89%). Furthermore, the growth rate ratio is higher with increasing variation in the maximal oxidative capacity as can be seen in Table 7. This result highlights a problem with targeting a specific growth rate as a control objective, as it requires accurate determination of the maximal value. This is a difficult task due to the uncertain nature of bioprocesses, as parameter variation depends on several factors such as the variation in operating conditions between batches. If the maximal growth rate is under estimated, the resulting suboptimal biomass productivity is lower than the desired one. If the maximal growth rate is overestimated, a regulation at 90% of this value could lead to acetate accumulation and metabolic switches, and thereby a growth inhibition.

On the other hand, regulating the acetate concentration and maintaining it at a low value offers a better practical trade-off, since the accumulation is avoided, and the obtained growth rate is consistent in the case of model mismatch. This is an interesting result since the acetate regulation approach is robust towards the change in operating conditions, and is not specific to the bacterial strain. The strategy could be applied to a different strain while ensuring the same level of performance without the need to estimate μ_{max} accurately.

9. Conclusions

In this paper, a robust Generic Model Control scheme is presented and applied to regulate the acetate concentration in *E. coli* BL21 (DE3) fed-batch cultures. The pro-

posed controller is based on feedback input-output linearization of the nonlinear model dynamics. A mechanistic model based on overflow metabolism is considered in the design phase. Due to the uncertain nature of the model, a robust design procedure using the $\mathcal{LMI}$ formalism is carried out, to compensate the model mismatch, disturbances, and measurement noise. Performance constraints are also formulated with $\mathcal{LMI}$s to ensure desired properties of the closed-loop transient response. The controller performance and robustness are validated through a series of simulations. The controller manages to stabilize the uncertain system near the optimal operating conditions despite unmodeled dynamics and external disturbances. Since the controlled variable (acetate) is not available for on-line measurement, a state estimation algorithm is required and an Unscented Kalman Filter (UKF) is implemented. The UKF is tuned based on experimental data, and validated both in simulation runs and in real-time experimental conditions. Finally, fed-batch experiments with a lab-scale reactor are performed in order to validate the efficiency of the coupled GMC-UKF strategy in driving the cultures near the optimal operating conditions.

Although the presented approach is suboptimal, it provides a practical solution to avoid overflow metabolism, since accurate measurements of the substrate concentration at the critical level are not possible. Furthermore, the strategy is not restricted to the studied strain since accurate determination of the maximal growth rate is not required. It is also adaptable to different control objectives such as substrate regulation at high concentrations in order to promote the product formation.

An improvement of the proposed control scheme is tracking a successively decreasing set-point calculated by numerical on-line optimization based on the estimation of the maximal growth rate. An experimental validation of this approach in future works could improve the process productivity since it provides a good trade-off between practicality and best achievable sub-optimality.

References

[1] S. Pontrelli, T.-Y. Chiu, E. I. Lan, F. Y.-H. Chen, P. Chang, and J. C. Liao, "Escherichia coli as a host for metabolic engineering," *Metabolic Engineering*, vol. 50, pp. 16–46, 2018.

[2] S. Y. Lee, "High cell-density culture of escherichia coli," *Trends in Biotechnology*, vol. 14, no. 3, pp. 98–105, 1996.

[3] G. W. Luli and W. R. Strohl, "Comparison of growth, acetate production, and acetate inhibition of Escherichia coli strains in batch and fed-batch fermentations," *Applied and Environmental Microbiology*, vol. 56, no. 4, pp. 1004–1011, 1990, ISSN: 00992240.

[4] K. Han, H. C. Lim, and J. Hong, "Acetic acid formation in escherichia coli fermentation," *Biotechnology and Bioengineering*, vol. 39, no. 6, pp. 663–671, 1992, ISSN: 10970290.

[5] M. Van De Walle and J. Shiloach, "Proposed mechanism of acetate accumulation in two recombinant Escherichia coli strains during high density fermentation," *Biotechnology and Bioengineering*, 1998, ISSN: 00063592.

[6] H. Crabtree, "Observations on the carbohydrate metabolism of tumours," *Biochem J*, vol. 23, pp. 536–545, 1929.

[7] D. Riesenberg, V. Schulz, W. Knorre, H.-D. Pohl, D. Korz, E. Sanders, A. Roß, and W.-D. Deckwer, "High cell density cultivation of escherichia coli at controlled specific growth rate," *Journal of Biotechnology*, vol. 20, no. 1, pp. 17–27, 1991.

[8] S. A. Rothen, M. Sauer, B. Sonnleitner, and B. Witholt, "Growth characteristics of escherichia coli hb101[pgec47] on defined medium," *Biotechnology and Bioengineering*, vol. 58, no. 1, pp. 92–100, 1998.

[9] B. W. Srinivasan, B. Sedghi, and D. Bonvin, "Terminal-cost optimization of a class of hybrid systems," *European Control Conference (ECC)*, vol. 09, pp. 3167–3172, 2001, ISSN: 00992240.

[10] I. Rocha, "Model-based strategies for computer-aided operation of a recombinant e. coli fermentation," Ph.D. dissertation, Universidade do Minho, Braga, 2003.

[11] S. Valentinotti, B. Srinivasan, U. Holmberg, D. Bonvin, C. Cannizzaro, M. Rhiel, and U. von Stockar, "Optimal operation of fed-batch fermentations via adaptive control of overflow metabolite," *Control Engineering Practice*, 2003, ISSN: 09670661.

[12] S. Jana and J. K. Deb, "Strategies for efficient production of heterologous proteins in Escherichia coli," in *Applied Microbiology and Biotechnology*, vol. 67, Springer Verlag, 2005, pp. 289–298.

[13] X. Hulhoven, F. Renard, S. Dessoy, P. Dehottay, P. Bogaerts, and A. Vande Wouwer, "Monitoring and control of a bioprocess for malaria vaccine production," *IFAC Proceedings Volumes*, vol. 39, no. 9, pp. 143–148, 2006.

[14] L. Dewasme, D. Coutinho, and A. Vande Wouwer, "Adaptive and robust linearizing control strategies for fed-batch cultures of microorganisms exhibiting overflow metabolism," in *Lecture Notes in Electrical Engineering*, vol. 89 LNEE, Springer, Berlin, Heidelberg, 2011, pp. 283–305, ISBN: 9783642195389.

[15] L. Dewasme, B. Srinivasan, M. Perrier, and A. Vande Wouwer, "Extremum-seeking algorithm design for fed-batch cultures of microorganisms with overflow metabolism," *Journal of Process Control*, vol. 21, no. 7, pp. 1092–1104, 2011.

[16] L. Santos, L. Dewasme, D. Coutinho, and A. Vande Wouwer, "Nonlinear model predictive control of fed-batch cultures of micro-organisms exhibiting overflow metabolism: Assessment and robustness," *Computers & Chemical Engineering*, vol. 39, pp. 143–151, 2012, ISSN: 0098-1354.

[17] K. Gonzalez, S. Tebbani, F. Lopes, A. Thorigné, S. Givry, D. Dumur, and D. Pareau, "Regulation of lactic acid concentration in its bioproduction from wheat flour," *Control Engineering Practice*, vol. 54, pp. 202–213, 2016.

[18] M. Jenzsch, R. Simutis, and A. Luebbert, "Generic model control of the specific growth rate in recombinant escherichia coli cultivations," *Journal of Biotechnology*, vol. 122, no. 4, pp. 483–493, 2006.

[19] M. Abadli, L. Dewasme, S. Tebbani, D. Dumur, and A. Vande Wouwer, "Generic model control applied to E. coli BL21(DE3) Fed-batch cultures," *Processes*, vol. 8, no. 7, p. 772, Jul. 2020, ISSN: 22279717.

[20] G. L. Kleman and W. R. Strohl, "Acetate metabolism by Escherichia coli in high-cell-density fermentation," *Applied and Environmental Microbiology*, 1994, ISSN: 00992240.

[21] S. Pinhal, D. Ropers, J. Geiselmann, and H. De Jong, "Acetate metabolism and the inhibition of bacterial growth by acetate," *Journal of Bacteriology*, 2019, ISSN: 10985530.

[22] P. Lee and G. Sullivan, "Generic model control (gmc)," *Computers & Chemical Engineering*, vol. 12, no. 6, pp. 573–580, 1988.

[23] M. DeLisa, H. Chae, W. Weigand, J. Valdes, G. Rao, and W. Bentley, "Generic model control of induced protein expression in high cell density cultivation of escherichia coli using on-line gfp-fusion monitoring," *Bioprocess and Biosystems Engineering*, vol. 24, no. 2, pp. 83–91, Sep. 2001.

[24] D. J. Costello, P. L. Lee, and P. F. Greenfield, "Control of anaerobic digesters using Generic Model Control," *Bioprocess Engineering*, 1989, ISSN: 0178515X.

[25] P. L. Douglas, P. S. Fountain, G. R. Sullivan, and W. Zhou, "Model based control of a high purity distillation column," *The Canadian Journal of Chemical Engineering*, 1994, ISSN: 1939019X.

[26] I. Rocha and E. Ferreira, "Model-based adaptive control of acetate concentration during the production of recombinant proteins with e. coli," *IFAC Proceedings Volumes*, vol. 35, no. 1, pp. 461–466, 2002, 15th IFAC World Congress.

[27] G. Bastin and D. Dochain, "On-line estimation and adaptive control of bioreactors," *Analytica Chimica Acta*, 1991, ISSN: 00032670.

[28] C. Retamal, L. Dewasme, A. L. Hantson, and A. Vande Wouwer, "Parameter estimation of a dynamic model of Escherichia coli fed-batch cultures," *Biochemical Engineering Journal*, vol. 135, pp. 22–35, Jul. 2018, ISSN: 1873295X.

[29] B. Sonnleitner and O. Käppeli, "Growth of saccharomyces cerevisiae is controlled by its limited respiratory capacity: Formulation and verification of a hypothesis," *Biotechnology and Bioengineering*, vol. 28, no. 6, pp. 927–937, 1986.

[30] L. Dewasme, G. Goffaux, A. L. Hantson, and A. Vande Wouwer, "Experimental validation of an Extended Kalman Filter estimating acetate concentration in E. coli cultures," in *Journal of Process Control*, vol. 23, Feb. 2013, pp. 148–157.

[31] E. Peter and L. Lee, *Nonlinear Process Control: Applications of Generic Model Control*. London Ltd. UK: Springer-Verlag, 1993.

[32] A. Isidori, M. Thoma, E. D. Sontag, B. W. Dickinson, A. Fettweis, J. L. Massey, and J. W. Modestino, *Nonlinear Control Systems*, 3rd. Berlin, Heidelberg: Springer-Verlag, 1995, ISBN: 3540199160.

[33] W. Zhou, P. L. Lee, and G. R. Sullivan, "Robust stability analysis of generic model control," *Chemical Engineering Communications*, vol. 117, no. 1, pp. 41–72, 1992.

[34] M. Chilali and P. Gahinet, "H_∞ design with pole placement constraints: An LMI approach," *IEEE Transactions on Automatic Control*, 1996, ISSN: 00189286.

[35] R. Wood, "Automatic control systems," *Water Research*, 1972, ISSN: 00431354.

[36] P. Bogaerts and A. Vande Wouwer, "Parameter identification for state estimation - Application to bioprocess software sensors," *Chemical Engineering Science*, 2004, ISSN: 00092509.

[37] S. J. Julier and J. K. Uhlmann, "New extension of the Kalman filter to nonlinear systems," in *Signal Processing, Sensor Fusion, and Target Recognition VI*, 1997, ISBN: 0819424838.

[38] ——, "Unscented filtering and nonlinear estimation," in *Proceedings of the IEEE*, 2004.

[39] L. Dewasme, S. Fernandes, Z. Amribt, L. O. Santos, P. Bogaerts, and A. Vande Wouwer, "State estimation and predictive control of fed-batch cultures of hybridoma cells," *Journal of Process Control*, vol. 30, pp. 50–57, 2015, ISSN: 09591524.

[40] J. F. Sturm, "Using sedumi 1.02, a matlab toolbox for optimization over symmetric cones," *Optimization methods and software*, vol. 11, no. 1-4, pp. 625–653, 1999.

[41] M. Müller, W. Meusel, U. Husemann, G. Greller, and M. Kraume, "Application of heat compensation calorimetry to an E. coli fed-batch process," *Journal of Biotechnology*, vol. 266, pp. 133–143, Jan. 2018, ISSN: 18734863.

[42] L. Dewasme, A. Richelle, P. Dehottay, P. Georges, M. Remy, P. Bogaerts, and A. Vande Wouwer, "Linear robust control of s. cerevisiae fed-batch cultures at different scales," *Biochemical Engineering Journal*, vol. 53, no. 1, pp. 26–37, 2010.

[43] I. Rocha, A. Veloso, S. Carneiro, E. Ferreira, and R. Costa, "Implementation of a specific rate controller in a fed-batch E. coli fermentation," in *IFAC Proceedings Volumes (IFAC-PapersOnline)*, 2008, ISBN: 9783902661005.

[44] H. De Battista, J. Picó, and E. Picó-Marco, "Nonlinear PI control of fed-batch processes for growth rate regulation," *Journal of Process Control*, 2012, ISSN: 09591524.